Spectroscopic studies of Cu^{2+} ion doped in $CaO\text{-}SrO\text{-}Na_2O\text{-}B_2O_3$ glasses

J. LAKSHMI KUMARI[a,b], V. NAGA PADMINI[a], J. SANTHAN KUMAR[a], SANDHYA COLE[a,*]
[a]*Department of Physics, Acharya Nagarjuna University, Nagarjuna Nagar, Guntur- 522 510, India*
[b]*Department of Physics, Y.A. Govt. Degree College for Women, Chirala- 523 155, India*

Glasses of the (20-x)CaO-xSrO-(20-y)Na_2O-60B_2O_3-y (CSNB) system with ($5 \le x \le 15$) mol% and y=0.1mol% of CuO were characterized by X-ray diffraction (XRD), EPR (Electron Paramagnetic Resonance), Optical absorption Spectra and FT-IR Studies. The EPR results indicate that the transition metal ions are present in octahedral site with tetragonal distortion. Spin-Hamiltonian parameters were evaluated. The Optical band energy (E_{opt}) and Urbach energy (ΔE) were calculated from their ultra violet edges. By correlating EPR and Optical data the molecular orbital coefficients have been evaluated. The IR studies shows that the glassy system contains BO_3 and BO_4 units in the disordered manner.

(Received March 16, 2012; accepted September 20, 2012)

Keywords: EPR, Optical absorption spectra, Borate glasses, Cu^{2+}ions, FT-IR

1. Introduction

Glasses play an important role in solid state electronic and ionic devices. Borate glasses are of great interest due to their structures and properties which are different from other glasses. Borate glasses are mainly used in electro-optic switches, electro-optic modulators, lasing materials and non-linear optical converters. Many researchers have studied B_2O_3 intensively in recent years [1,2], since they are relatively easy to obtain and moreover present interesting structural particularities, due to the existence of the boron anomaly. The boron atom can be placed in the network in tri-or tetra co-ordination depending on the concentration of the modifier oxide [3 – 6]. B_2O_3 is one of the most important glass forming oxides and has been incorporated into various kinds of glass systems in order to obtain different physical and chemical properties [7]. Transition metal ions are being mostly used in the recent years to find the glass structure, since their outer d-electron orbital function has a broad radial distribution and due to their high sensitive response to the changes in the surrounding actions. Among various transition metal ions, the copper ion, a Para-magnetic metal ion, when dissolved in glass compositions in very small quantities makes the glasses colored and has a strong influence over the optical properties of the glasses [8]. The studies of transition metal ions in glasses by EPR and optical absorption techniques give information on the structure of the glass. In different glasses copper can exist as a monovalent Cu^{+} ion or as divalent Cu^{2+} ion to be sensitive to the glass environment. In the present study preparation and characterization of (20-x)CaO-xSrO-(20-y)Na_2O-60B_2O_3-y (CSNB) glasses were done by using EPR, and optical absorption and IR studies.

2. Experimental

The glass samples were prepared by the melt quenching method with the composition given in Table 1. The materials used in the present study are Analar grade B_2O_3 (99.9 %), CaO (99.9 %), $SrCO_3$ (99.9 %) and Na_2CO_3 (99.9 %). For transition metal doping 0.1 mol % of CuO (99.9 %) is added to the starting materials. These mixtures are sintered at 500^{o} C and melt in an electric furnace in porcelain crucible at 900^{0}C - 1000^{0}C for nearly 1 hr. The melt is then quenched at room temperature in air to form a glass. The glasses so formed are annealed at 300^{0}C for about 1hr. X-ray powder diffraction patterns of glass samples were recorded using Copper target on Philips PW (1710) diffractomer at room temperature. EPR recordings were made at room temperature on JEOL-JM FE3 with 100 KHz field modulation 100 EPR spectrometer Optical absorption spectra are recorded at room temperature on JASCO V670 Spectrophotometer in 200-900 nm. Infrared transmittance spectra of the powdered glass samples were recorded using JASCO FT-IR 5300 Spectrometer in the wave number range 400-4000 cm^{-1} at room temperature.

Table 1. Composition (mol%) of the glasses studied in the present work.

Glass Code	CaO	SrO	Na_2O	B_2O_3	CuO
$CSNB_0$	15	5	20	60	--
$CSNB_1$	5	15	19.9	60	0.1
$CSNB_2$	10	10	19.9	60	0.1
$CSNB_3$	15	5	19.9	60	0.1

3. Results and discussion

3.1 XRD

The X-ray powder diffraction data for two glass systems were obtained from Central Instrumentation Lab, HCU, Hyderabad, India and is shown in Fig. 1. The Philips PW 1710 X-ray powder Diffractometer was used. The results were recorded using a PM 8208A chart recorder and an A100 (Digital) printer with VT125 terminal simultaneously. X-ray diffraction technique was used to check for possible crystallinity of the sample after quenching and annealing. The samples were found to be completely amorphous in nature.

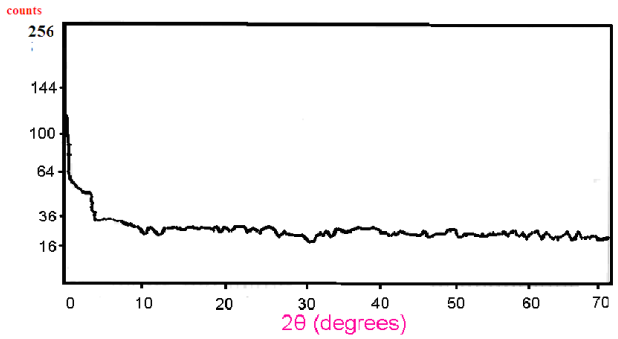

Fig. 1 XRD Spectrum of CSNB glass system.

3.2 EPR study

No EPR signal is observed in undoped glasses confirming that the starting materials used in the present work were free from transition metal impurities. When Cu^{2+} ions were added to the CSNB glass systems the EPR spectra exhibited resonance signals similar to those reported for Cu^{2+} ions in Na_2O-B_2O_3, Na_2O-K_2O-B_2O_3 glass systems [9, 10]. The Cu^{2+} ion with S = ½ has a nuclear spin I = 3/2 for both ^{69}Cu (the natural abundance 69%) and ^{65}Cu (natural abundance 31%) and therefore (2I+1) i.e., four parallel and four perpendicular hyperfine components would be expected. In the observed spectra, three parallel components were observed in the lower field region. The perpendicular components in the higher field region were well resolved. The EPR spectra of the three glass systems doped with Cu^{2+} ions are shown in Fig. 2. The spectrum closely resembles that of the Cu^{2+} ion in most oxide glasses [11,12] from the spectral analysis the spin-Hamiltonian parameters are calculated using the equation [13] and are presented in Table 2. From Table 2, it is clear that $g_{\parallel} > g_{\perp} > g_e$ i.e., Cu^{2+} is in an octahedral coordination with tetrahedral distortion and the ground state of Cu^{2+} is $d_{x^2-y^2}$. Also $g_{\parallel}$ and $g_{\perp}$, $A_{\parallel}$ and $A_{\perp}$ (B_1=40, B_2=46, B_3=53) values increases with the composition by varying CaO and SrO content in CSNB glasses systems and $g_{\parallel}$ reaches a maximum for x= 15% SrO, and x = 5% CaO and then reaches a minimum for x = 10% CaO and x = 10% SrO in CSNB glass system. Thus from Fig.2, Table 2, it is clear that the EPR spectra of (20-x)CaO-xSrO-(20-y)Na_2O-60B_2O_3-yCuO glasses systems were strongly concentration dependent. The EPR spectra were analyzed using the spin-Hamiltonian

$$H = g_{\parallel} \beta Hz S_z + g_{\perp} \beta (H_x S_x + H_y S_y) + A_{\parallel} S_z I_z + A_{\perp} (S_x I_x + S_y I_y) \quad (1)$$

Here Z is the symmetry axis, β, is the Bohr magneton, S and I are the electron and nuclear spin operators, H_x, H_y and H_z are the static magnetic field components, $g_{\parallel}$ and $g_{\perp}$ are the parallel and perpendicular components of the hyperfine tensor A. The values of $A_{\parallel}$ are calculated using the following equation due to Kivelson [14] from Table 2. It is clear that $g_{\parallel}$ and $g_{\perp}$ values increases slightly and reach a minimum in CSNB glasses at about 15% CaO. $g_{\parallel}$ and $g_{\perp}$ values increase abruptly and reaches a maximum at about 10% CaO and 10% SrO. It is also clear from Table 2, that $A_{\parallel}$ value decreases with decrease of CaO and there is considerable increase in $A_{\perp}$ at about 5% CaO and 15% SrO. This indicates that the distortion around Cu^{2+} ion is changing with the decreasing content of CaO and increasing content of SrO, and also indicates a continuous structural change in the glass systems.

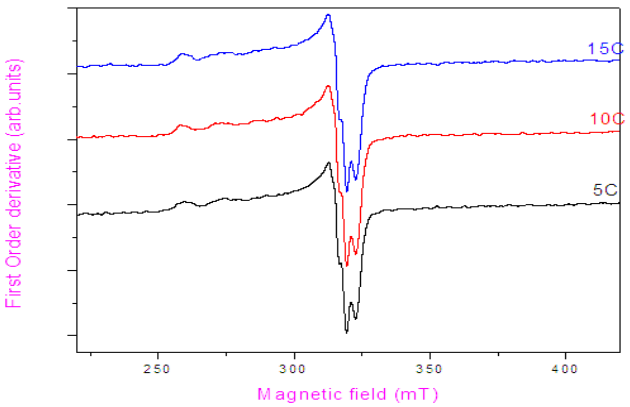

Fig. 2. EPR Spectrum of Cu^{2+} doped CSNB glass systems.

Table 2. Comparison of spin-Hamiltonian parameters of Cu^{2+} ions in different systems.

System	$g_{\parallel}$	$g_{\perp}$	$A_{\parallel}$ x 10^{-4} (Cm^{-1})	Reference
Na_2O- B_2O_3	2.327	2.065	150	9
Na_2O- K_2O-B_2O_3	2.338	2.046	135	10
CaO-SrO-Na_2O- B_2O_3(1)	2.329	2.066	117	Present work
CaO-SrO-Na_2O- B_2O_3(2)	2.335	2.055	123	Present work
CaO-SrO-Na_2O- B_2O_3(3)	2.351	2.056	130	Present work

3.3 Optical absorption spectrum

Optical absorption spectra for all glass composition exhibit a single broad peak (Fig. 3) in the range 715-750 nm, which can be attributed to the presence of Cu^{2+} ion in the glass [15]. This absorption can be assigned to the $^2E_g(D) \rightarrow {}^2T_{2g}(D)$ transition of Cu^{2+} ion, by varying CaO and SrO content the optical absorption peak range shifted towards higher wavelength region. The absorption peak position of CSNB glasses at different concentration of CaO and SrO are given in Table 3, similar results were reported in literature [16-19]. Experimental data shows that the cupric ion generally exists in solutions solids and glasses in octahedral symmetry with a strong tetragonal distortion [16-20]. According to the present EPR studies Cu^{2+} ions in CSNB glasses present in octahedral symmetry with elongated tetragonal distortion.

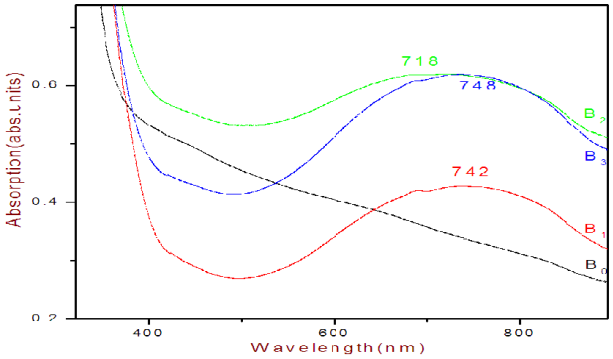

Fig. 3. Optical bands of Cu^{2+} doped CSNB glass systems.

Table 3. Absorption peak of Cu^{2+} bonding parameters and % of bonding symmetry of Cu^{2+} doped in CaO-SrO-Na_2O- B_2O_3 glasses.

Sample	Cu^{2+} peak (nm)	Γ_σ (%)	Γ_π (%)	α^2	β_1^2	β	K
$CSNB_1$	742	61.22	16	0.719042857	0.923148195	0.960806013	0.3703
$CSNB_2$	718	57.09	12	0.737995237	0.948542021	0.973931219	0.3458
$CSNB_3$	748	57.52	10	0.736014285	0.952889383	0.976160531	0.3337

3.4 Optical basicity

The Optical basicity of an oxide glass will reflect the ability of glass to donate negative change to the probe ion [21]. Duffy and Ingram [22] proposed that the optical basicity can be predicted from the composition of the glass and basicity moderating parameters of various cations present. The theoretical values of the optical basicity (Λ_{th}) of the glasses can be calculated using the following formula,

$$\Lambda_{th} = \sum_{i=1}^{n} \frac{Z_i r_i}{|Zo|\gamma_i} \quad (2)$$

where 'n' is the number of cations present 'Z'$_i$ is the oxidation number of the ith cation, 'r$_i$' is the ratio of number of ith cation to the number of oxides present and 'γ_i' is the basicity moderating parameters, of the ith cation. The basicity moderating parameters 'γ_i'' can be calculated from the following equation.

$$\gamma_I = 1.36 \quad (x_i \quad - \quad 0.26) \qquad (3)$$

where 'x_i' is Pauling electro negativity of the cation. The theoretical values of the optical basicity (Δ_{th}) of all the glass samples were calculated and are presented in Table 4. It is observed that with the increase SrO and decrease of CaO content the value of optical basicity increases.

Table 4. Summary of Direct, Indirect, Urbach energies and Optical Basicity.

Sample	Direct	Indirect	Urbach	Optical basicity
$CSNB_0$	3.968	3.882	0.257	0.5374
$CSNB_1$	3.763	3.724	0.269	0.5369
$CSNB_2$	3.749	3.699	0.270	0.5388
$CSNB_3$	3.719	3.690	0.271	0.5405

3.5 Optical energy and Urbach energy

The values of the optical energy gap and Urbach energy calculated in the present work for different glasses are presented in Table 4 and is shown in Fig. 4,5,6. The values obtained in the present work are of the same order for those of copper tellurium oxide [23] and borate glasses [24]. From the values of the widths of the tails of the localized states (Δ E) within the optical band gap for the present glasses, it can be observed that the direct and indirect values increases and Urbach energy values decreases. The decrease in Urbach energy with Cu^{2+} concentration can be considered as due to decreased defects [25].

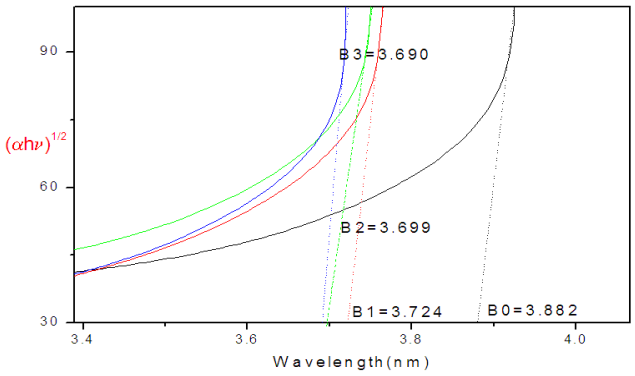

Fig. 4. Indirect bands of Cu^{2+} doped CSNB glass systems.

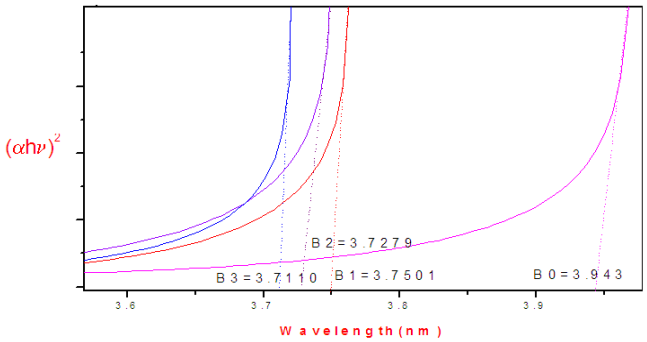

Fig. 5. Direct bands Cu^{2+} doped CSNB glass systems.

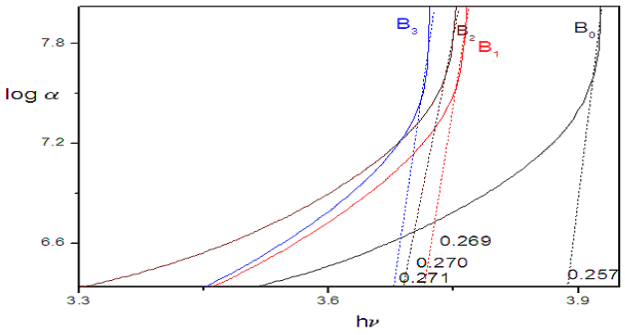

Fig. 6. Urbach energy bands of Cu^{+2} doped CSNB glass systems.

3.6 Molecular Orbital coefficients

The EPR and optical absorption data can be correlated to evaluate the bonding coefficients as follows [19]

$$g_{II} = 2.0023 \left[1- \frac{4 \lambda \alpha^2 \beta_1^2}{E_1} \right] \qquad (4)$$

$$g_{\perp}=2.0023 \left[1- \frac{\lambda \alpha^2 \beta_1^2}{E_2} \right] \qquad (5)$$

where λ, spin orbit coupling parameter is equal to -828 cm^{-1} for CuO and $\beta^2 \approx 1$ for octahedral environment. ΔE_{xy} (E_1) and $\Delta E_{xz,yz}$ (E_2) are heights of the d_{xy} and $d_{xz,yz}$ and molecular orbital levels above the ground state d_{x2-y2} and these values are estimated from optical absorption spectra [26]. In optical absorption spectra the position of observed absorption maximum of Cu^{2+} ions indicates the value of ΔE_{xy} from Table 3. It is observed that the bonding parameters are changing with the percent of CaO and SrO. The bonding co-efficient α^2, β_1^2 and β characterize respectively. The in plane σ bonding in-plane $\prod$ bonding and out of plane $\prod$ bonding of the copper (II) complex their values lie between 0.5 and 1.0 the limits of pure covalent and pure ionic bonding [27] The value of the calculated α^2, β_1^2 indicate that the in plane σ bonding is covalent. The normalizes covalency of Cu-O in–plane bonding of σ and $\prod$ symmetry are expressed by [28] in terms of bonding coefficients α^2, β_1^2 as

$$\Gamma_\sigma = \frac{200(1-S)(1-\alpha^2)}{1-2S} \quad \% \qquad (6)$$

$$\Gamma_\prod = 200\,(1-\beta_1^2)\,\% \qquad (7)$$

where s is the overlap integral (S_{oxy} = 0.076). The normalized covalency values of the Cu (II) – O of in–plane bonding of $\prod$ symmetry ($\Gamma_\prod$). The calculated are given in Table 3. The bonding coefficient α^2 (in- plane σ bonding) can be calculated from the EPR data using the following expression given by Kuska et al [29].

$$\alpha^2 = \frac{7}{4}\left[\frac{A_{II}}{P} - \frac{A}{P} - \frac{2}{3}g_{II} - \frac{5}{21}g_{\perp} + \frac{6}{7}\right] \qquad (8)$$

where P = 0.036 cm^{-1} and A = ($1/3A_{II} + 2/3A_\perp$) the α^2 value calculated from the above equation was used in equation 10 and 11 to evaluate β_1^2 from the spin-Hamiltonian parameters the dipole term (P) and the Fermi-contact term (K) are calculated using the expressions [30, 31].

$$P = 2\gamma_{Cu}\,\beta_0\,\beta_N\,(r^{-3}) = 0.036\ cm^{-1} \qquad (9)$$

$$K = (A_0/P) + \Delta g_0 \qquad (10)$$

Here γ_{Cu} is the magnetic moment of copper, β_0 is the Bohr magneton, β_N is the nuclear magneton and r is the distance from the central nucleus to the electron.

$A_o = (A_{II} + 2A_\perp)/3$, where A_{II} and $A_\perp$ are the hyperfine coupling constants in the parallel and perpendicular directions to the field. g_{II} and $g_\perp$ are the g-values parallel and perpendicular to the field and $\Delta g_0 = g_0 - g_e$, where $g_0 = (g_{II} + 2g_\perp)/3$ and g_e is the free ion (g_e.= 20023). The Fermi contact term K is a measure of the polarization produced by the uneven distribution of d-electron density on the inner core s-electron. The evaluated values of K (Table 3) are tune with the general order of [32].

3.7 FT- IR studies

Usually the vibrational modes of the borate network are found [33] to be active in three infrared spectral regions, which are similar to those reported by several workers. First group bands was reported to occur at 1200-1600cm^{-1} and is due to the asymmetric stretching relaxation of the B-O band of trigonal BO_3 units, whereas second group lies between 800 and 1200 cm^{-1} and is due to the B-O band stretching of the tetrahedral BO_4 units. Finally the third group is observed around 700 cm^{-1} and is attributed to bending of B-O-B linkages in the borate networks. The principal frequencies observed in the IR spectrum of the glasses studied and their assignments are summarized in Table 5 and is shown in Fig. 7. The spectra corresponding to glasses of systems containing the absorption bands of the vitreous B_2O_3 There is the band at ~700-713 cm^{-1} assigned to the B-O-B deformation vibrational mode [34, 35]. The band at ~ 951 cm^{-1} characteristic of glasses with high B_2O_3 content is due to boroxol rings [36]. Its intensity diminished, when X = 10 % CaO and X = 10 % SrO content. The band at 1006 - 1016cm^{-1} is assigned to the B-O stretching mode including tetra-coordinated boron atoms (BO_4). The intensity of this band increase when X= 15% SrO concentration increases. Around 1207-1249 cm^{-1} a band assigned to the B-O stretching including three coordinated boron atoms (BO_3), [34-38]. By comparing the amplitude of bands at ~ 1016 cm^{-1} and ~ 1249 cm^{-1}. The dominant presence of the BO_4 units as compared to the BO_3 units is obvious. Around ~ 1360 cm^{-1} a shoulder belonging to the 1249 cm^{-1} band of the boroxol rings was identified. The appearance of the H-O-H bending mode centered at 1726 cm^{-1} proves the hygroscopic character of the glasses investigated. The intensity of this band increases when X = 5% CaO and X =15% SrO content of the sample. The absorption band at around 2847-2920 cm^{-1} can be attributed to the hydrogen bonds. The same peaks have been recorded [33]. In the 3410-3431 cm^{-1} spectral a broad band assigned to the H-O stretching mode (hydrogen bonded) was identified. The band around 1410-1419 cm^{-1} containing diborate groups Very weak absorption band is observed at 472 cm^{-1} when X = 5 % CaO tentatively assigned to CaO_4 tetrahedra on the basis of a vibrational study of various crystalline calcium compounds CaO_4 tetrahedra give bands in the 400 – 500 cm^{-1} region. The observations made in the present investigation agree with the literature values [8, 39-41]. The structural changes may be explained by the partial replacement of oxygen atoms by varying CaO and SrO content.

Table 5. FT-IR studies.

Wave number (Cm^{-1})			Assignment
$CSNB_1$	**$CSNB_2$**	**$CSNB_3$**	
472	--	--	Ca-O Stretching mode
609	--	--	Sr-O Stretching mode
713	700	717	B-O-B deformation Vibrational mode
951	--	951	Boroxol ring vibration
1014	1016	1006	B-O stretching mode of BO_4 units
1149	--	--	B-O stretching mode of BO_3 units
--	--	1207	B-O stretching mode of BO_3 units
--	--	1249	B-O stretching mode of BO_3 units
1419	1410	1415	B-O-B deformation mode
--	--	1726	H-O-H bending mode
--	2847	2851	H-O-H bending mode
--	2918	2920	H-O-H bending mode

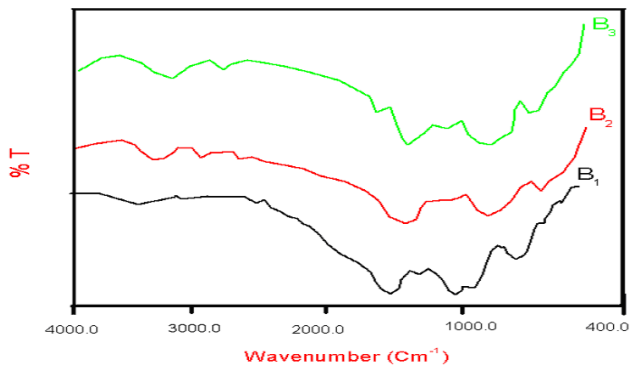

Fig. 7. FT-IR Spectra of Cu^{+2} doped CSNB glass systems.

4. Conclusions

1. From the EPR and Optical spectra of Cu^{2+} ions in CSNB glasses, it is confims that the copper ions occupied octahedral sites with tetragonal distortion.
2. The structural changes takes place with decreasing CaO and increasing SrO composition.
3. The optical absorption spectra of these samples gives single broad band due to Cu^{2+} ions in distorted octahedral sites.
4. FT- IR studies shows that the glassy system contains BO_3 and BO_4 units in the disordered manner.
5. The optical band gaps direct, indirect and Urbach energies are found to vary with CaO and SrO content which is assigned to the increase in defect concentration with CuO content.
6. By Correlating EPR and optical data, the molecular orbital coefficients α^2, β_1^2 are evaluated. The values suggest that the in - plane σ bonding is moderately covalent in nature.

Acknowledgement

One of the authors (J. Lakshmi Kumari, letter No. F. ETFA PANO. 84 / FIP-XI Plan) is thankful to UGC, New Delhi for providing financial assistance under FDP Programme to carry out these investigations.

Dr. Sandhya Cole would like to thank the University Grants Commission, New Delhi for Sanctioning UGC-MRP F. No. 9-498/2010(SR).

References

[1] Eskisehir, G. U. Journal of Science **22**(3), 129 (2009).
[2] G. Lakshminarayana, S. Buddhudu, Spectrochim, Acta, part A, **63**(2), 295 (2006).

[3] I. Tawansi, A. Gohar, D. Holland, N. A. E-I. Shishatawi, J. Phys and Apply. phys. **21**, 607 (1988).
[4] H. Ushida, Y. Iwadate, T. Hattori, S. Nishiyama, K. Fukushima, Y. Ikeda, M. Yamaguchi, M. Misawa, T. Fukunaga, T. Nakazawa, S. Jitsukawa, J. Alloys Compounds **377**, 167 (2004).
[5] T. Takaishi, J. Jin, M. Takaishi, T. Uchino, T. Yoko. Proc. Int. Congrs. Glass. 2. Extended Abstracts. Edenburgh. Scotland, 1-6 (2001).
[6] I. Yasui, H. Hasegawa, Y. Saito, Y. Akasaka, J. Non-Cryst. Solids. **123**, 71 (1990).
[7] T. Yana, N. Kunimine, S. Shibata, M. Yamane, J. Non-Cryst. Solids. **321**, 147 (2003).
[8] G. Upender, V. Kamalaker, C. P. Vardhani, V. Chandra Mouli, Indian Journal of pure and Applied Physics. **47**, 551 (2009).
[9] R. V. S. S. N. Ravi Kumar, V. Raja gopal Reddy, A. V. Chandra Sekhar, B. J. Reddy, Y. P. Reddy , P. S. Rao, Journal of Alloys and Compounds. **337**, 272 (2002).
[10] R. P. Sreekanth Chakradhar, K. P. Ramesh, J. L .Rao, J. Rama Krishna, J. Phys. Condens, Matter **15**, 1469 (2003).
[11] S. Suresh, J. Chinna Babu, V. Chandra Mouli, Phys. Chem (Italic) Glasses, **46**, 27 (2005).
[12] J. D. Lee Concise inorganic chemistry (Black well Science, Oxford) (1996).
[13] J. M. Dance, J. Drmaudery, H. Baudry, M. Moneraya, Solid State Comm, **39**, 199 (1981).
[14] D. Kivelson, Lee-SK, J. Chem. phys, **47**, 11 (1986).
[15] S. Sakka, K. Kamira, K. Makita, Yamanoto, J. Non-Cryst. Solids. **63**, 223 (1984).
[16] T. Bates, in "Modern Aspects of the Vitreous State", edited by J. D. Mackenzie (Butter Worths, London) **2**, 195 (1962).
[17] R. Harani, C. A. Hogarth, K. A. K. Lott. J. Mater. Sci, **19**, 1420 (1984).
[18] I. Ardelean, O. Cozar, S. Filip, V. Pop, I. Cenan Solid State Commun **100**, 609 (1996).
[19] R. R. Kumar, A. K. Bhatnagar, B. C. V. Reddy, Solid State Commun. **114**, 493 (2000).
[20] A. Klonkowski, Phy. Chem . Glasses, **24**, 116 (1983).
[21] A. J. Easteal, A. T. Marcom, J. Non-cryst. Solids **34**, 29 (1979).
[22] J. A. Duffy, M. D. Ingram, J. Inorg. Nul. Chem. **37**, 1203 (1975).
[23] M. A. Hassan, C. A. Hogarth, J. Mater Sci. **23**, 2500 (1988).
[24] A. I. Sabry, M. M. E-Samanoudy, J. Mater Sci, **30**, 3930 (1995).
[25] M. Vithal, P. Nachimuthu, T. Banu, R. Jagannathan, J. Apply. Phys. **81**, 7922 (1997).
[26] Krosh-Moe, J. phys. Chem .Glasses, **6**, 46 (1965).
[27] A. Klonkowski, Phys. Chem. Glasses, **24**, 116 (1983).
[28] H. Kawazoe, H. Hosono, T. Kanazawa, J. Non Cryst Solids, **33**, 103 (1979).
[29] H. A. Kuska, M. T. Rogers, R. E. Durllinger, J. Phys. Chem. **71**, 109 (1967).
[30] D. Kivelson, R. Neiman, J. Chem. phys **35**, 149 (1961).
[31] K. E. Folk, E. Ivanova, B. Roos, T. Vanogard, Inorg. chem. **9**, 556 (1970).
[32] J. H. Vanveleck, Phys. Rev. **41**, 208 (1932).
[33] S. G. Motke, S. P. Yawale, S. S. Yawale, Bull Mater. Sci. **25**, 75 (2002).
[34] F. F. Bentley, L. D. Smithson, A. L .Rozee, Infrared Spectra and Characteristic Frequencies 700- 300 cm^{-1}.
[35] B. Sharma, D. Dubc, A. Mansingh, J. Non-Cryst . Solids, **69**, 39 (1984).
[36] C. S. Sundandana, R. Singh, Phys. Status Solidi (A) K91 (1983).
[37] E. Culea, I. Bratu, A. L. Nicula, ibid, 83, K 15 (1984).
[38] C. N. R. Rao "Chemical Applications of Infrared spectroscopy" (Academic press. Newyork) (1963).
[39] I. Ardelean, M. Peteanu, R. Ciceo-Lucacel, Journal of Material Science, Materials in Electronics **11**, 11 (2000).
[40] S. Suresh, M. Prasad ,G. Upender, V. Kamalaker, V. Chandra Mouli, Indian Journal of pure and Applied Physics **47**, 163 (2009).
[41] N. Srinivasa Rao, M. Purnima, Shashidhar, Bale, K. Siva Kumar, Syed Rahman, Bull. Mater Sci, **29**, 365 (2006).

*Corresponding author: sandhya.cole@gmail.com